Available online at www.sciencedirect.com
ScienceDirect
Journal of Catalysis 243 (2006) 309–317
JOURNAL OF CATALYSIS
www.elsevier.com/locate/jcat

The effect of proximity between Pt and BaO on uptake, release, and reduction of NO_x on storage catalysts

Noel W. Cant *, Irene O.Y. Liu, Michael J. Patterson

Department of Chemistry and Biomolecular Sciences, Macquarie University, NSW 2109, Australia

Received 12 May 2006; revised 21 July 2006; accepted 29 July 2006

Available online 15 September 2006

Abstract

In this study, we compared the NO_x storage reduction characteristics of four systems: BaO/Al_2O_3 alone, a sequential system with Pt/SiO_2 ahead of the BaO/Al_2O_3, a combined system with the Pt/SiO_2 and BaO/Al_2O_3 physically mixed, and BaO/Al_2O_3 with Pt deposited on it. We also investigated the isotopic exchange between ^{15}NO and stored NO_x under storage conditions for the latter two systems. The rate of exchange was more than five times as fast for $Pt/BaO/Al_2O_3$ than for the combined $Pt/SiO_2 + BaO/Al_2O_3$ system, demonstrating spillover of NO_x species between Pt and BaO in close proximity. Movement of NO_x in this way can also explain why storage from NO/O_2 reached completion much faster for $Pt/BaO/Al_2O_3$ than for the sequential or combined systems, where the influence of Pt was confined to the oxidation of NO to NO_2 with storage by disproportionation to nitrate and NO alone. The initial product of the decomposition of stored NO_x in He was NO_2 with the sequential system and NO with the combined system, where Pt in the same bed decomposed NO_2. However, NO_2 in excess of the NO_2/NO equilibrium ratio was seen during release of stored NO_x from $Pt/BaO/Al_2O_3$, reflecting transfer back to the metal, which was deactivated for NO_2 decomposition by high oxygen coverage. A large fraction of the NO_x stored on $Pt/BaO/Al_2O_3$ was immediately converted to N_2 alone when exposed to H_2, with formation of NH_3 evident only after H_2 breakthrough. This is consistent with the reduction of stored NO_x species as they transfer back to Pt particles. Reduction in the combined system requires considerably higher temperature and forms NH_3 as the major product. This is consistent with the decomposition of stored NO_x to gaseous NO_x and subsequent reduction by a catalytic reaction on Pt particles located remotely from BaO. In the sequential system, reduction was largely confined to the conversion of NO_2 to NO. Measurement of the O:N ratio in the products formed by temperature-programmed decomposition showed that NO was stored on BaO/Al_2O_3 in the presence of O_2 as a species with the formula NO_2. Similar measurements with NO_2, which is stored in much larger quantities, were consistent with conversion to nitrate, in agreement with existing knowledge.

Keywords: NO_x storage; $Pt/BaO/Al_2O_3$; BaO/Al_2O_3; Pt/SiO_2; Proximity; ^{15}N exchange

1. Introduction

The use of storage/reduction catalysts based on combinations of Pt and BaO to mitigate NO_x emissions from lean-burn, direct-injection gasoline engines was first described in the technical literature in 1995 [1,2] and has since seen limited use on vehicles sold in Japan and elsewhere. There is general agreement as to the way in which the components work in unison. During lean operation, the platinum oxidizes NO to a mixture of NO and NO_2 (NO_x), which is stored on the barium component as various NO_x species (nitrate, nitrite, nitro). A short period of rich operation then leads to NO_x mobilization and reduction, again on Pt or other platinum group metals, if present. However, as described in the review by Epling et al. [3], there is a diversity of opinion as to the details of both the storage and reduction steps. In part, this diversity is due to the different conditions adopted by researchers. Studies emulating vehicle operation typically use complex mixtures and rapid cycling, which can disguise the details of the chemistry. On the other hand, much spectroscopic information has been gathered under conditions (e.g., uptake at room temperature, followed by slow stepwise reaction in different atmospheres at higher temperatures) that may lead to the formation of species not necessarily relevant to vehicle operation.

There is good evidence that BaO/Al_2O_3 free of Pt takes up NO_2 more readily than NO [4,5] and that NO_2 storage is char-

* Corresponding author. Fax: +61 2 9850 8313.
E-mail address: noel.cant@mq.edu.au (N.W. Cant).

0021-9517/$ – see front matter
doi:10.1016/j.jcat.2006.07.030

acterized by an initial period of complete uptake, followed by a more prolonged period of partial uptake with liberation of NO [6–11] as an accompaniment to the disproportionation of NO_2 to stored nitrate, that is,

$$3NO_2 + O^{2-} \rightarrow 2NO_3^- + NO. \quad (1)$$

The presence of Pt modifies this process, because the NO liberated can be reoxidized to NO_2. Oxidation of NO to NO_2 plays a substantial role in NO_x storage from NO/O_2 mixtures on $Pt/BaO/Al_2O_3$, but additional processes involving spillover from the metal may be present [4,7,12].

The reduction cycle is generally described as desorption of gaseous NO_x, induced by temperature [13,14] and/or by CO_2 [15,16] and other compositional changes as oxidized species are removed [3], followed by reduction of the NO_x to N_2 and other products on Pt or other noble metal particles [17–20]. However, it is difficult to decouple these steps [3], and reduction by spillover routes have also been discussed [21,22].

Four recent studies have addressed the reduction question in detail. In a follow-up to their earlier study of the Pt system alone [20], Abdulhamid et al. [23] compared H_2, CO, C_3H_6, and C_3H_8 for reduction of NO_x stored from NO_2 alone on BaO/Al_2O_3 containing Pt, Pd, or Rh. Their results showed that H_2 and CO are more efficient reductants than either hydrocarbon, especially for the $Pt/BaO/Al_2O_3$ system, in which NH_3 is a low-temperature product. Szailer et al. [24] investigated H_2, CO, and a mixture of the two as reductants of NO_x stored on Pt/Al_2O_3 and on $Pt/BaO/Al_2O_3$, again from NO_2, using in situ FTIR and XRD measurements. Reduction by H_2 was observed at temperatures as low as 420 K and explained in terms of a complex temperature-dependent mechanism that included removal of oxygen atoms from Pt, direct reduction of stored NO_x, and formation of NCO groups that underwent hydrolysis to NH_3 and reaction with desorbing NO_x. Nova et al. [25,26] studied storage and H_2 reduction on BaO/Al_2O_3 (from NO_2) on $Pt/BaO/Al_2O_3$ (from NO/O_2) and on physical mixtures of Pt/Al_2O_3 and BaO/Al_2O_3 and concluded that reduction of the nitrate formed on $Pt/BaO/Al_2O_3$ occurred not by liberation of gaseous NO_x and reduction elsewhere, but rather by a Pt-catalyzed surface reaction involving one or more types of spillover processes.

The present work is similar to that of Nova et al. [25,26] in that we have investigated the importance of close contact between Pt and BaO through comparison of catalyst systems in which the two components are arranged differently. In our case, we studied four arrangements and used Pt/SiO_2 rather than Pt/Al_2O_3 in physical mixtures to eliminate the known adsorption of NO_x on alumina [27]. We also investigated NO_x spillover directly through the determination of the rate of exchange between ^{15}NO and stored $^{14}NO_x$ for two of the systems. The results confirm and extend the findings of Nova et al. [25,26].

2. Experimental

Storage, release, and reduction measurements were carried out with four sample arrangements. The first of these arrangements comprised 50 mg of BaO/Al_2O_3 alone. The BaO content [i.e., $BaO/(BaO + Al_2O_3)$] was 15.5 wt%, equivalent to a loading (i.e., BaO/Al_2O_3) of 18.3 wt%. The second arrangement was a sequential bed arrangement with 50 mg of 1.1 wt% Pt/SiO_2 packed upstream of 50 mg of the same BaO/Al_2O_3 preparation. The third was a combined bed containing 50 mg of the same Pt/SiO_2 uniformly mixed with 50 mg of the BaO/Al_2O_3. The fourth was 50 mg of 1 wt% $Pt/BaO/Al_2O_3$ made by impregnating the BaO/Al_2O_3 with platinum. Thus, all four arrangements were identical in terms of BaO content, and the three Pt-containing arrangements had similar weights of Pt.

The Pt/SiO_2 was part of the batch designated as 40-SiO_2-PtCl-L in the series prepared and characterized by Uchijima et al. [28]. It was made by impregnation of silica (Davison grade 62; 285 m^2/g; particle size, 180–210 μm) with an aqueous solution of H_2PtCl_6 and contained 1.1 wt% Pt with a dispersion of 40% after reduction at 300 °C, as determined by H_2 chemisorption and XRD line broadening [28,29].

The BaO/Al_2O_3 samples were from a single batch prepared as described previously [30] by three successive incipient wetness impregnations of an industrial washcoat-grade alumina (Condea; particle size, 4–10 μm; BET surface area, 140 m^2/g; pore size, ∼10 nm) using a barium acetate solution. Before and after each impregnation, the preparation was dried at 100 °C and calcined in flowing 10% O_2/He at 400 °C. The resultant fine powder was pressed, crushed, and sieved to a particle size of 106–180 μm.

The platinum-containing variant was prepared by a further incipient wetness impregnation with a solution of $Pt(NH_3)_4(NO_3)_2$ at a concentration set to produce a loading of 1.0 wt%. The dispersion of platinum in the sample used for NO_x experiments, as estimated by H_2 chemisorption after reduction in 2500 ppm H_2 in He on a ramp ending with 50 min at 550 °C, was ∼66%. The chemisorption was carried out at 45 °C from a stream containing a rather low hydrogen concentration (5000 ppm H_2 in 500 ppm Ar/He) to minimize uptake on the support. XRD measurements showed a very weak broad line at $2\Theta = 39.8°$, the position expected for the Pt(111) reflection. The particle size, estimated from the apparent line width using the Scherrer equation, was ∼9 nm, equivalent to a dispersion of ∼12%, but the line shape could not be defined with sufficient accuracy to exclude the presence of a high percentage of smaller particles. The principal components of the XRD pattern were broad lines attributable to the starting amorphous alumina (largely δ-form) and sharper lines attributable to rather large particles (20–30 nm) of the witherite phase of $BaCO_3$.

Samples were tested in a flow system as described previously [8]. The system comprised a 4-mm-i.d. quartz reactor with upstream and downstream switching values to enable analysis of the product or bypass stream by three methods: mass spectrometry (Balzers Thermostar model GSD 300T) every 4 s, chemiluminescent analysis (Ecotech model 9841) for NO and NO_2 every 12 s, and gas chromatography (MTI model M200 with molecular sieve and Poraplot U columns) every 100 s. The sensitivity was ∼1 ppm for all components except H_2 on the gas chromatograph, for which it was limited to ∼100 ppm. The samples were packed between layers of quartz wool with an

additional thin layer of the wool between the Pt/SiO_2 and the BaO/Al_2O_3 in the sequential-bed arrangement. Each sample was freed of carbonaceous contaminants by one or more exposures to 500 ppm NO_2 in 3% O_2/He at 360 °C, followed by ramping to 600 °C in He. The total flow rate was set at 100 cm^3 (STP)/min throughout, a GHSV of ∼100,000 h^{-1}.

Processing of the mass spectrometer signal at m/z of 30 to obtain NO concentrations required careful correction for fragmentation of NO_2, which changed in response to large changes in the concentrations of NO_2 and O_2. The procedure used was to allow the correction factor to adjust exponentially after the change to a new value based on normalization against the NO reading from the chemiluminescent analyzer as soon as this was stable. Such adjustment was not required during isotope exchange determinations, because these were carried out using the standard steady-state isotope transient kinetic analysis (SSITKA) procedure [31] with NO, NO_2, and O_2 concentrations all constant after storage reached steady state. Exchange was followed by monitoring signals with m/z of 30 (^{14}NO), 31 (^{15}NO), 46 ($^{14}NO_2$), and 47 ($^{15}NO_2$). The ^{15}NO was obtained from Isotec Inc. with a stated purity of 99.6% ^{15}N, but analysis showed ∼4% $^{14}N^{16}O$ and 3.3% $^{15}N^{18}O$ as impurities. It was made up in a small cylinder as a 1% mixture in 1% Ar/He and arranged so that this mixture could be switched back and forth in place of the standard mixture of 1% ^{14}NO in helium using a low volume 1/16-inch four-ported valve (Valco, Inc.). The resultant step rise in the Ar signal was complete in <3 s.

3. Results and discussion

3.1. Storage of NO on BaO/Al_2O_3

Uptake of NO on the BaO/Al_2O_3 material when using a 600-ppm NO in 3% O_2/He feed proceeded as illustrated in Fig. 1A. In this figure, and in Figs. 2–4, mass spectrometry analyses are shown as lines; chemiluminescent analyses, by small open symbols; and gas chromatography analyses, by larger open symbols. The argon signal is normalized to the concentration of NO_x ($NO + NO_2$) on bypass. As can be seen, a short period (∼54 s) of complete NO uptake was followed by a steep rise in NO concentration, with the bypass concentration reached in less than 1000 s. Activity for the oxidation of NO to NO_2 was negligible throughout. Similar curves for the uptake of NO in O_2/He on BaO/Al_2O_3 have been reported by Nova et al. [5,32,33].

Subsequent temperature-programmed decomposition (TPD) of the stored NO_x (Fig. 1B) gave two maxima in NO production. The first maxima (at ∼380 °C) was without concurrent production of O_2, and the second (at ∼560 °C) was accompanied by O_2 at approximately three-quarters of the NO concentration. The overall molar ratio of O:N in all the material driven off [i.e., $(2O_2 + NO + 2NO_2)/(NO + NO_2)$] was ∼2. Thus, the species stored corresponds, at least on average, to NO_2 rather than to NO. The release of NO in two regimes, one accompanied by oxygen and the other not accompanied by oxygen, can

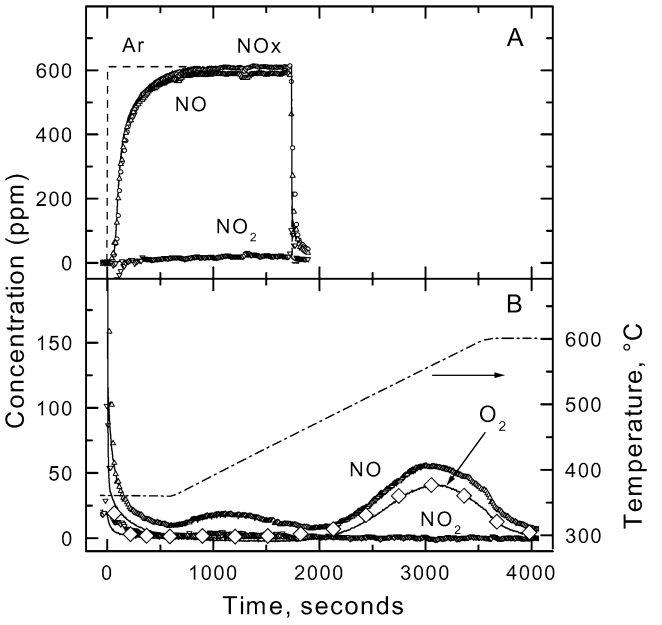

Fig. 1. Storage of NO followed by TPD decomposition of stored NO_x on 50 mg of BaO/Al_2O_3: (A) storage from 600 ppm NO in 3% O_2/He at 360 °C followed by (B) TPD on a ramp at 5 °C/min.

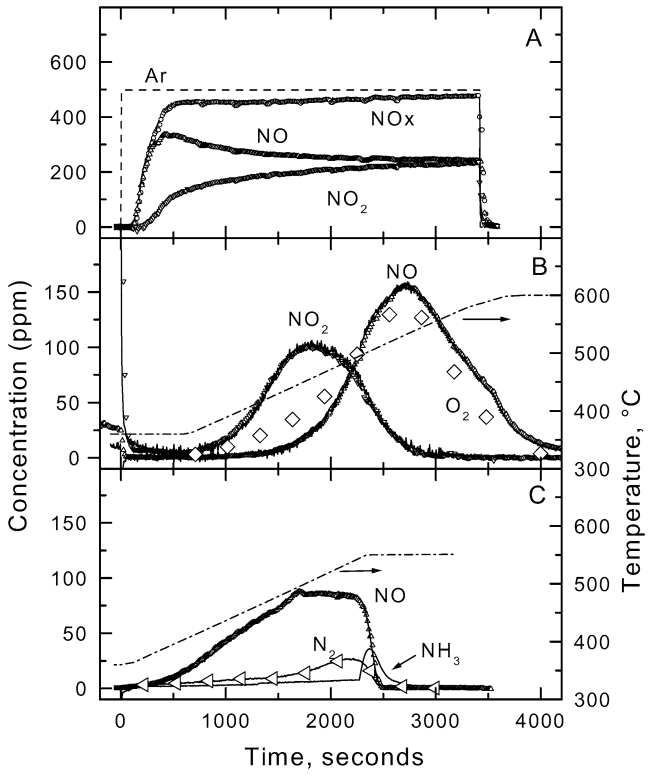

Fig. 2. Storage of NO_x followed by TPD or TPR of stored NO_x for the sequential bed comprising 50 mg of 1 wt% Pt/SiO_2 followed by 50 mg of BaO/Al_2O_3: (A) storage at 360 °C using a feed of 500 ppm NO in 3% O_2/He, (B) TPD of NO_x stored using a feed of 500 ppm NO_2 in 3% O_2/He, (C) TPR of NO_x stored from NO/O_2 as per (A) above in 2500 ppm H_2/He.

be explained if a sorbed NO_2 species decomposes in two stages, initially by disproportionation to surface nitrate and NO,

$$3NO_2\,(a) + O^{2-} \rightarrow 2NO_3^- + NO, \qquad (2)$$

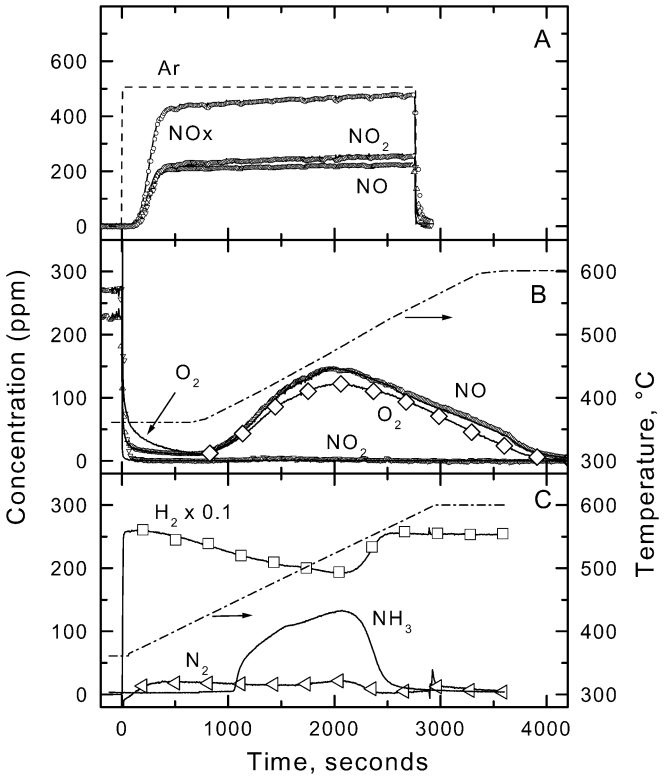

Fig. 3. Storage of NO_x followed by TPD or TPR of stored NO_x for a combined bed comprising 50 mg of 1 wt% Pt/SiO_2 mixed with 50 mg of BaO/Al_2O_3: (A) storage at 360 °C using a feed of 500 ppm NO in 3% O_2/He, (B) TPD of NO_x stored using a feed of 500 ppm NO_2 in 3% O_2/He, (C) TPR of NO_x stored from NO/O_2 as per (A) above in 2500 ppm H_2/He.

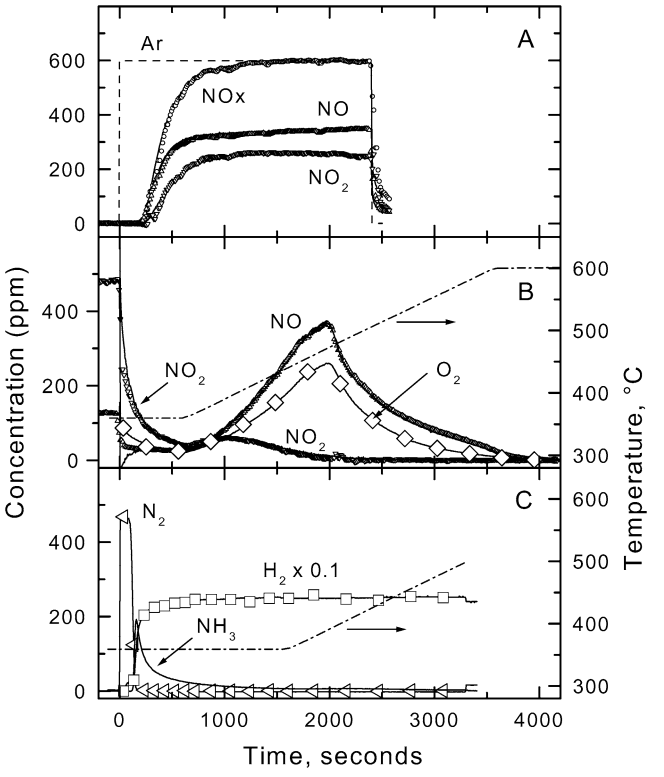

Fig. 4. Storage of NO_x followed by TPD or TPR of stored NO_x for 50 mg of $Pt/BaO/Al_2O_3$: (A) storage at 360 °C using a feed of 600 ppm NO in 3% O_2/He, (B) TPD of NO_x stored using a feed of 500 ppm NO_2 in 3% O_2/He, (C) TPR of NO_x stored from NO/O_2 as per (A) above in 2500 ppm H_2/He.

followed by decomposition of the surface nitrate according to

$$2NO_3^- \rightarrow 2NO + 1.5O_2 + O^{2-}. \quad (3)$$

Step (1) may be facilitated by generation of gaseous NO_2, which readsorbs on sites adjacent to other neighboring adsorbed NO_2 species downstream. We have observed a similar release of NO in two stages in the ratio of 1:2 after storage of NO_2 on BaO/Al_2O_3 at 300 °C, but only when TPD was started before the emergence of NO_x [30]. If the storage was extended beyond the breakthrough of NO_2, then further uptake of NO_2 was accompanied by oxidation via disproportionation to nitrate and generation of NO. TPD of the resultant stored nitrate still gave two peaks, but the first peak was no longer NO alone, but rather NO_2 and O_2 at a ratio of 4:1. The sequential bed with Pt present to oxidize NO to NO_2 ahead of the BaO storage component exhibited this behavior, as shown below.

Two types of experiments were carried out for each of the three Pt-containing catalyst systems. One of these comprised uptake at 360 °C from a feed containing NO_2 in O_2/He, followed by isothermal desorption in He for 600 s and then TPD. The second involved uptake from NO in O_2/He at 360 °C and isothermal desorption in He for 600 s, followed by TPR in H_2/He. Because the initial activity of the Pt in each system was more than sufficient to equilibrate NO with NO_2 to an equilibrium mixture of the two, similar uptakes are expected regardless of the nitrogen oxide used. Figs. 2–4 show the storage data obtained when using NO/O_2 alone. As commented upon below, small differences were apparent for some catalyst arrangements due to deactivation of Pt when directly exposed to NO_2.

3.2. Storage and reduction for the sequential bed system

Fig. 2A shows the storage uptake behavior using NO/O_2 for the sequential catalyst system with Pt/SiO_2 ahead of BaO/Al_2O_3. With this arrangement, NO was oxidized to an equilibrium mixture of NO/NO_2 before striking the BaO/Al_2O_3. The period of complete uptake (∼105 s) was much longer than for storage from NO in O_2/He on BaO/Al_2O_3 alone in Fig. 1A. Also, unlike that system, uptake from the NO/NO_2 mixture continued over thousands of seconds, with the NO concentration exceeding the final equilibrium concentration for some time after the initial breakthrough. As noted earlier, generation of NO is characteristic of the storage of NO_2 on BaO/Al_2O_3, which occurs with disproportionation to surface nitrate according to Eq. (1).

Storage of NO_2/O_2 on the sequential-bed arrangement (not shown) was similar to that of NO, except that the direct exposure of the Pt/SiO_2 to NO_2 led to a gradual loss of oxidation activity. As a result, the final NO/NO_2 ratio was considerably less than the near 1:1 ratio shown in Fig. 2A. Continuous deactivation of a Pt/Al_2O_3 catalyst for the decomposition of NO_2 alone has been reported by Olsson and Fridell [34] and attributed to the formation of platinum oxide on the basis of XPS measurements. Very recent detailed kinetic studies of NO oxi-

dation on Pt also document strong inhibition by NO_2 and lower rates when oxygen coverages are high [35].

TPD of the NO_x stored from NO_2 in O_2/He (Fig. 2B) produced partially overlapping peaks of NO_2 (and some O_2) at ~455 °C and then NO (accompanied by considerably more O_2) at ~532 °C, consistent with the presence of two types of NO_x species, one of which decomposes with a stoichiometry of

$$2NO_3^- \rightarrow 2NO_2 + 0.5O_2 + O^{2-} \quad (4)$$

and the other according to Eq. (3). The O:N ratio in the products, integrated over both peaks, was ~2.5, as expected for the decomposition of a metal nitrate to its oxide. These characteristics are typical of those observed during decomposition of NO_x stored from NO_2 on Pt-free BaO/Al_2O_3 systems [4,8,25,26,36–39]. Szanyi et al. [38] presented evidence showing that the species giving rise to NO_2 are nitrates bound to a monolayer of BaO and that bulk-like nitrates are producing NO. However, the detailed modeling of NO_x storage and TPD by Olsson et al. [7] and extended by Scotti et al. [40] paints a more complex picture. According to the five-step reversible model used, NO_2 is liberated when barium nitrate decomposes, but NO is formed if NO_2 readsorbs on free BaO sites when they are created downstream and subsequently decomposes at a higher temperature.

Decomposition of NO_x (stored from NO/O_2) in the presence of 2500 ppm H_2 in He (Fig. 2C) gave mainly NO due to reduction of NO_2,

$$NO_2 + H_2 \rightarrow NO + H_2O, \quad (5)$$

as we reported previously for NO_x stored from NO_2 on BaO/Al_2O_3 alone [37] and confirmed in recent work by Nova et al. [25,26]. The concentrations of NO_2 and O_2 (not shown) were negligible (<2 and <5 ppm, respectively). Some N_2 and NH_3 was produced with maximum evolution rates at 539 and 550 °C (the end of the ramp), respectively. The peak shape for NH_3, with a sharp initial rise, was distorted by the presence of some adsorption before breakthrough.

3.3. Storage and reduction for the combined-bed system

With the combined system (equal weights of Pt/SiO_2 and BaO/Al_2O_3 blended in the same bed), uptake from NO in O_2/He (Fig. 3A) was similar to that for the sequential system in terms of the breakthrough time (~116 s), the slow approach of the total NO_x concentration to the bypass value, and a final NO/NO_2 ratio near equilibrium. However, the initial overshoot in NO concentration during the partial uptake in Fig. 2A was absent. Thus, although storage by disproportionation was almost certainly the major process, one of its characteristic features, NO release, was disguised by the continual conversion of this NO to NO_2 on the Pt/SiO_2 within the bed. The data of Nova et al. [25,26] for a physical mixture of Pt/Al_2O_3 and BaO/Al_2O_3 are quite similar.

With the combined bed, uptake from NO_2 in O_2/He (not shown) was identical to that from NO in O_2. The only nitrogen oxide liberated during the subsequent TPD in He (Fig. 3B) was NO, accompanied by three-quarters of its concentration of O_2 rather than NO_2 first and then NO, as was observed for the sequential bed (Fig 2B). The difference again can be attributed to the presence of Pt/SiO_2 in the bed, causing near-complete decomposition of NO_2 to NO,

$$2NO_2 \rightarrow 2NO + O_2. \quad (6)$$

Decomposition is favored thermodynamically because O_2 concentrations during TPD are very low (<120 ppm, or 0.012%, vs 3% during uptake). The data of Nova et al. [25,26] for a physical mixture of Pt/Al_2O_3 and BaO/Al_2O_3 are quite similar but show evolution of a small amount of NO_2 and an O_2/NO ratio below the 0.75 expected for Eq. (3).

As shown in Fig. 3C, ammonia was the major product when NO_x, stored on the combined bed, was subjected to TPR in H_2/He. The concentrations of all nitrogen oxides, NO, NO_2, and N_2O, were negligible (<2 ppm) after H_2 was switched in. Generation of NH_3 probably commenced at the same temperature as H_2 consumption (well below 400 °C), but its appearance was delayed by adsorption of the initial amounts formed. Subsequent desorption of this material is then the reason why the NH_3 concentration peaked at a temperature above that at which the evolution of NO reached a maximum in Fig. 3B. The TPR data of Nova et al. [25,26] for H_2 reduction of NO_x stored on a physical mixture of Pt/Al_2O_3 and BaO/Al_2O_3 is quite similar in terms of both NH_3 and N_2 production.

Ammonia formation is characteristic of the catalytic reaction between NO and H_2 over Pt catalysts under particular conditions. Previous work with the same Pt/SiO_2 used here [41,42] has shown that the products of this reaction are almost entirely N_2 and N_2O in approximately equal amounts at 360 °C when the H_2/NO ratio in the feed is low (e.g., 0.5), which is sufficient only for completion of the reactions

$$2NO + 2H_2 \rightarrow N_2 + 2H_2O \quad (7)$$

and

$$2NO + H_2 \rightarrow N_2O + H_2O. \quad (8)$$

Under these conditions NH_3 comprised <1% of the products; however, NH_3 became dominant (~96% of all nitrogen-containing products) when the H_2/NO ratio was sufficient (i.e., 2.5) for the reaction

$$2NO + 5H_2 \rightarrow 2NH_3 + 2H_2O. \quad (9)$$

Thus, the formation of NH_3 during TPR is consistent with decomposition of the NO_x stored on BaO/Al_2O_3 particles to gaseous NO and NO_2, which diffuse to neighboring Pt/SiO_2 particles, where they undergo reduction to NH_3 under conditions in which the H_2/NO ratio is very high.

Steady-state experiments in which a low concentration of NO was reacted over the combined bed in the presence of 2500 ppm H_2 showed complete conversion of NO at 360 °C, with formation of ~84 ppm of NH_3 and 5 ppm of N_2 from ~95 ppm of NO. Similarly, the reaction of ~130 ppm of NO at 450 °C yielded ~113 ppm of NH_3 and ~8 ppm of N_2. Formation of N_2O was negligible (<2 ppm) at both temperatures. The ratio of N_2 to NH_3 during reduction of stored NO_x stored on $Pt/BaO/Al_2O_3$ was somewhat higher, with concentration maxima of 20 and 120 ppm, respectively (Fig. 3C). This may be

due to the generation of locally high concentrations of NH_3 in the periphery of Pt/SiO_2 particles, which can then react with incoming NO molecules to form N_2 by the SCR reaction

$$6NO + 4NH_3 \rightarrow 5N_2 + 6H_2O, \quad (10)$$

for which the Pt/SiO_2 used here gives complete conversions at temperatures above 220 °C [43].

3.4. Storage and reduction for $Pt/BaO/Al_2O_3$

Storage of NO_x from NO/O_2 by the $Pt/BaO/Al_2O_3$ sample differed from that by the sequential and combined systems in two ways. First, the breakthrough time was almost twice as long: ∼214 s in Fig. 4A vs 105 and 116 s in Figs. 2A and 3A, respectively. Second, uptake, as judged by the approach of the NO_x concentration to the bypass concentration, did not continue indefinitely, but ceased after ∼1200 s. Thus, the rate of storage on $Pt/BaO/Al_2O_3$ is faster, and full total storage capacity under the conditions used is attained more quickly. The implication is that Pt, in close proximity to BaO, either allows uptake of NO or NO_2 in a way that is not feasible when Pt is absent or enables conversion of NO_x to nitrate as storage proceeds. Spillover of NO_2 from Pt to BaO/Al_2O_3 is one way in which the latter might occur. The data of Nova et al. [25,26] for their $Pt/BaO/Al_2O_3$ (1:20:100) sample are similar.

Storage from NO_2 in O_2/He (not shown) proceeded similarly as that of NO, except that the direct exposure of $Pt/BaO/Al_2O_3$ to NO_2 at the front of the bed led to a gradual decline in the activity for NO_2 decomposition to a greater extent than was apparent with the sequential- and combined-bed systems. As a result, the NO/NO_2 ratio when storage ceased was considerably less than that shown in Fig. 4A, where loss of activity was hardly noticeable. Some degree of deactivation for NO_2 decomposition was also apparent in the data of Nova et al. [32] for the storage of NO_2 alone on $Pt/BaO/Al_2O_3$. Much more rapid deactivation was reported by Olsson and Fridell [34] for the same system but using a catalyst with a very low Pt dispersion (∼0.01 by CO chemisorption). The deactivation of this $Pt/BaO/Al_2O_3$ was much faster than that of a comparison Pt/Al_2O_3 catalyst.

TPD of NO_x stored from NO_2 in O_2/He gave the results shown in Fig. 4B. As for the combined bed, NO evolution dominated as the ramp proceeded, consistent with the decomposition of NO_2 on Pt. Nonetheless, and unlike the combined bed, NO_2 evolved at concentrations higher than that of NO, much higher than equilibrium, during the isothermal stage and the initial part of the ramp. Thus, the activity of Pt was insufficient to decompose NO_2 completely, probably due to deactivation by the presence of high oxygen concentrations on its surface. Comparison of Fig. 4B and Fig. 3B also shows that the temperature giving the maximum rate of NO evolution for the $Pt/BaO/Al_2O_3$ system was similar to that for the combined $Pt/SiO_2 + BaO/Al_2O_3$ system. However, the peak NO concentration, and the fall-off in NO concentration at temperatures above the peak, was much steeper. Thus, close proximity between Pt and BaO facilitated removal of stored NO_x to some extent. The implication is reverse spillover of a NO_x species from the BaO component to Pt and desorption of NO or NO_2 from there. The data of Nova et al. [26] for decomposition of NO_x stored on $Pt/BaO/Al_2O_3$ also show a tail under isothermal conditions and an overwhelming dominance by NO during the ramp.

As is apparent from Fig. 4C, TPR of NO_x stored on $Pt/BaO/Al_2O_3$ from NO/O_2 proceeded very differently from that seen with the sequential- and combined-bed systems. Hydrogen was completely consumed for a considerable period after its introduction with N_2 as the nearly exclusive product. Evolution of NO (not shown) was almost entirely absent except for a small peak not exceeding 20 ppm after 25 s. The concentration of N_2 produced during this period (∼470 ppm) is close to the 500 ppm expected for complete consumption of the ∼2500 ppm H_2 in the feed through reduction of nitrate,

$$2NO_3^- + 5H_2 \rightarrow N_2 + O_2^- + 2H_2O. \quad (11)$$

If the surface NO_x species were nitrite or NO_2, then the expected concentrations would be 833 and 625 ppm, respectively, assuming that the following stoichiometries were applicable:

$$2NO_2^- + 3H_2 \rightarrow N_2 + 3H_2O + O^{2-} \quad (12)$$

and

$$2NO_2 + 4H_2 \rightarrow N_2 + 4H_2O. \quad (13)$$

The rapid conversion of stored NO_x to N_2 on $Pt/BaO/Al_2O_3$, alone among the systems studied here, can be explained in terms of rapid spillover of two possible types. One type is dissociation of H_2 on Pt with spillover of hydrogen atoms to react with NO_x bound to BaO. The alternative is that a NO_x species undergoes reverse spillover from the support to Pt and reacts with hydrogen atoms as they are formed by dissociation. In that situation, N_2 should be formed preferably to NH_3 if the ratio of H atoms to NO_x is low on the Pt surface. Removal of oxygen atoms from the Pt by reaction with hydrogen is a potential driving force for reverse spillover.

The data in Fig. 4C show a steep rise in ammonia production after unreacted H_2 appeared and the concentration of N_2 dropped to zero. Ammonia production exhibited a sharp peak with a prolonged tail that persisted during the subsequent temperature ramp. The likely explanation for this is that NH_3 was formed when NO_x, liberated from BaO too remote from Pt particles to benefit from spillover, reached Pt by diffusion through the gas phase and then reacted with H_2 according to reaction (9) in the same way as for the combined-bed system.

It may be noted here that although the H_2 concentration used in the present work was low, the reduction rate with $Pt/BaO/Al_2O_3$ was so fast that some increase in temperature due to the exothermicity of the reaction was feasible. This would increase the generation of gaseous NO_x to some extent and hence increase the rate of any remotely catalyzed component of the reaction. However, Nova et al. [25,26], in experiments under similar conditions, demonstrated that reduction started below 100 °C, when the heat release could not possibly produce a temperature high enough to decompose stored NO_x. On this basis, they argued strongly that reduction of NO_x stored on $Pt/BaO/Al_2O_3$ involves either NO_x spillover, as we favor here, or some other Pt-catalyzed process present only when the metal and oxide are in contact.

Table 1
NO_x released and stored (in mmol/g) at 360 °C

System	TPD after uptake from NO_2/O_2[a]		Uptake from NO/O_2	
	NO_2	NO	To breakthrough[b]	When complete[c]
Sequential	0.17	0.29	0.08	~0.35
Combined	<0.01	0.41	0.10	~0.40
$Pt/BaO/Al_2O_3$	–	–	0.20	~0.40

[a] Estimated by integration of NO and NO_2 peaks in Figs. 2B and 3B.
[b] Amount stored until the exit NO_x concentration exceeded 2% of the input concentration.
[c] Total amount taken up when exposure to NO/O_2 was terminated in Figs. 2A, 3A, and 4A.

Table 1 summarizes the amounts of NO_x stored from NO/O_2 and released during TPD in the immediately previous uptake from NO_2/O_2 when that was measured for the three Pt-containing systems. The total amounts stored on prolonged exposure were similar for each system, but the amount taken up by the $Pt/BaO/Al_2O_3$ system to the point of NO_x breakthrough was twice or more that for the sequential and combined systems. The NO_x/Ba ratios corresponding to total uptake were in the range 0.35–0.40, which is 18–20% of the theoretical capacity if full conversion to $Ba(NO_3)_2$ was possible. It was not possible to assess the amounts of N_2 and NH_3 formed during TPR with good accuracy, due to limitations associated with calibration of the mass spectrometer for NH_3 and in integrating product formation at low concentration (<10 ppm) over thousands of seconds.

3.5. Exchange between ^{15}NO and stored NO_x

Several of the foregoing findings point to the existence of forward and reverse spillover of NO_x species between Pt and BaO. This process was probed directly by measuring the rate of exchange between ^{15}NO and stored $^{14}NO_x$ for the $Pt/BaO/Al_2O_3$ and combined systems, as shown in Fig. 5. The experiments were carried out as per the standard SSITKA method [31] with the catalysts exposed to $^{14}NO/O_2$ until uptake was close to complete (3600 s) before the switch from ^{14}NO to ^{15}NO was made. Because the conditions were steady state and isothermal, with total NO, NO_2, and O_2 concentrations all constant, restrictions due to heat and mass transfer restraints of a chemical nature can be completely excluded.

With the combined system (Fig. 5A), the concentrations of ^{14}NO and $^{14}NO_2$ immediately dropped and then slowly trended to zero. Correspondingly, ^{15}NO and $^{15}NO_2$ first rose rapidly and then slowly plateaued. Thus, the pool of immediately exchangeable material was small, and exchange was spread over thousands of seconds.

The behavior of the $Pt/BaO/Al_2O_3$ catalyst (Fig. 5B) was quite different, with a delay before the ^{14}N species began to decline and the ^{15}N species appeared. The subsequent changeover between the species was fast, with steady-state concentrations reached in ~1000 s. Exchange was clearly much more rapid than in the combined system.

TPD of the combined system at the end of exchange gave the results shown in Fig. 6A. The amount of ^{15}NO driven off was somewhat greater than that of ^{14}NO. The concentrations of both $^{15}NO_2$ and $^{14}NO_2$ were low, reflecting near-complete decomposition to NO on the Pt, as shown in Fig. 3B. Based on the relative amounts of ^{15}N and ^{14}N species evolved, the fractional extent of exchange was 0.59. It is interesting to note that the concentration of ^{15}NO reached a maximum at a temperature somewhat lower than that for ^{14}NO. This indicates some heterogeneity in the stored NO_x (e.g., surface and bulk), with the latter exchanging after the former.

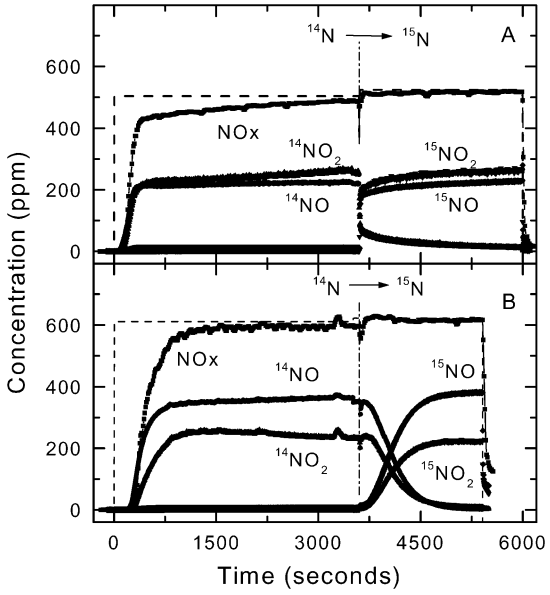

Fig. 5. $^{14}N/^{15}N$ exchange during storage at 360 °C using a NO/O_2/He feed: (A) for the combined bed comprising 50 mg of 1 wt% Pt/SiO_2 mixed with 50 mg of BaO/Al_2O_3 using a feed containing 500 ppm NO in 3% O_2/He, (B) for 50 mg of $Pt/BaO/Al_2O_3$ using a feed containing 600 ppm NO in 2% O_2/He.

The dominant product during TPD of the exchanged $Pt/BaO/Al_2O_3$ catalyst (Fig. 6B) was ^{15}NO. However, $^{15}NO_2$ was also significant in the initial stages. As noted previously in conjunction with Fig. 4B, it appears that in this system, Pt had limited activity for the decomposition of NO_2, presumably due to the presence of high concentrations of oxygen adatoms created during uptake when Pt and BaO were in contact. The concentrations of both ^{14}N species were very low, with an overall $^{15}N/(^{14}N + {}^{15}N)$ ratio equal to 0.96. This was close to complete exchange given that the ^{15}NO used contained ~4% ^{14}NO as an impurity.

The isotope-exchange data were further processed on the simple premise that exchange was first-order in the distance from complete exchange, that is,

$$\ln(1 - Z) = -kt, \tag{14}$$

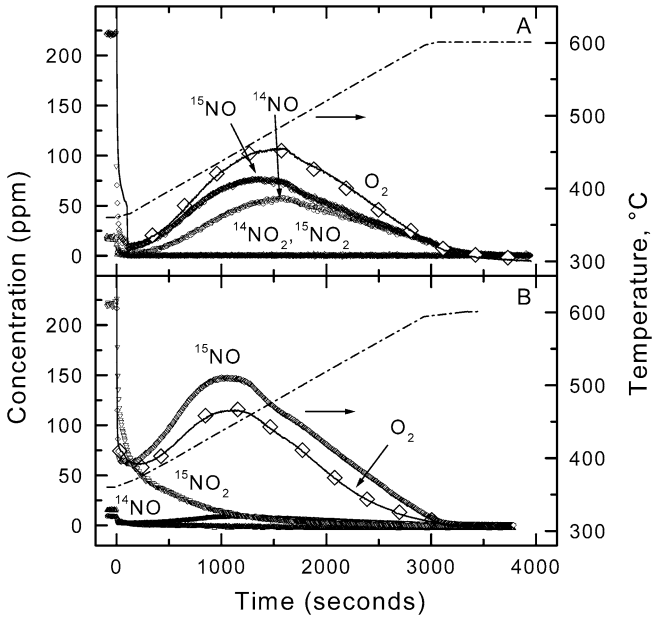

Fig. 6. TPD of stored NO_x at the conclusion of $^{14}N/^{15}N$ exchange at 360 °C as per Fig. 5: (A) for the combined bed comprising 50 mg of 1 wt% Pt/SiO_2 mixed with 50 mg of BaO/Al_2O_3 using a feed containing 500 ppm NO in 3% O_2/He: (B) for 50 mg of $Pt/BaO/Al_2O_3$ using a feed containing 600 ppm NO in 2% O_2/He.

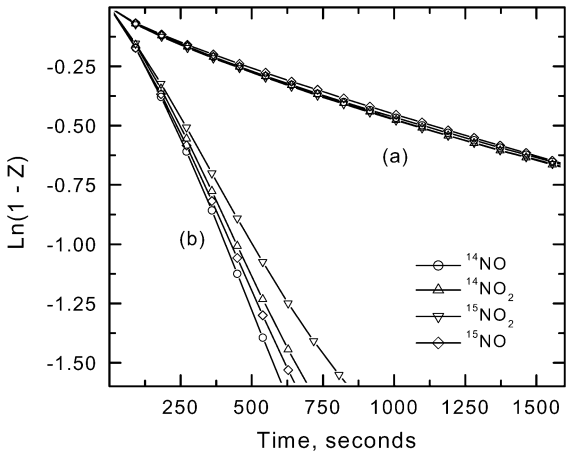

Fig. 7. First-order exchange plots as per Eq. (14) for $^{14}N/^{15}N$ exchange during storage at 360 °C as per Fig. 5: (a) for the combined bed comprising 50 mg of 1 wt% Pt/SiO_2 mixed with 50 mg of BaO/Al_2O_3 using a feed containing 500 ppm NO in 3% O_2/He, (b) for 50 mg of $Pt/BaO/Al_2O_3$ using a feed containing 600 ppm NO in 2% O_2/He.

where Z is the fraction of the total pool that has exchanged at time t. Fig. 7 shows plots of this type for the two systems studied here. For each of the four species, the fraction exchanged at any time was calculated from the data in Fig. 5 by cumulative sum of the quantities released into the feed stream (for ^{14}N species) or removed from it (for ^{15}N species) in the intervals between successive mass spectrometric analyses. These sums were then normalized based on the sum of that evolved (or removed) when the exchange was terminated and the known fractional conversion of stored $^{14}NO_x$ to $^{15}NO_x$ at that time (from the TPD results in Fig. 6). The plots in Fig. 7 show only every fifteenth point, to avoid overlapping of symbols.

As can be seen, the points (which cover the first 80% of the observed exchange) show good linearity, with reasonable agreement between the four species. The data for $^{14}NO_2$ should be the most reliable. That for the two ^{15}N species was less accurate, because the calculations require exact values for the final concentrations of ^{15}NO and $^{15}NO_2$, which are somewhat uncertain, because uptake still continued to a small extent. Determination of ^{14}NO (at $m/z = 30$) was less accurate than that of $^{14}NO_2$ (at $m/z = 46$) because of the uncertainty inherent in the rather large correction for $^{14}NO_2$ fragmentation.

The half-lives for exchange, based on the $^{14}NO_2$ data, are ~320 s for $Pt/BaO/Al_2O_3$ and ~1690 s for the combined system of Pt/SiO_2 and BaO/Al_2O_3. Thus, close proximity between Pt and BaO increased the apparent rate of exchange by a factor of ~5.3. This provides clear evidence in favor of migration of surface NO_x between Pt particles and BaO when they are co-located. In principle, it should be possible to improve the accuracy of the rate ratio through direct modeling of the individual steps involved; however, this is beyond the scope of the present study, given the complexity of the model needed to explain NO_x storage and TPD results [7,40] and the possibility that the exchange data for $Pt/BaO/Al_2O_3$ in Fig. 5B may be influenced by chromatographic effects in the initial stages [31].

Finally, it may be noted that there was no conflict between the rather rapid exchange evident with $Pt/BaO/Al_2O_3$ at 360 °C and the relative stability of NO_x species when TPD commenced at the same temperature as in Fig. 4B. Isotope exchange as investigated here is a measure of the steady-state rates of NO_x adsorption and desorption when all sites are occupied and NO_x concentrations are constant. In contrast, decomposition of stored NO_x into helium during TPD creates vacant sites on which gaseous NO_x can readsorb. Desorption/readsorption repeated many times is responsible for the apparent stability, as demonstrated by modeling of Gorte [44,45] and others.

4. Conclusion

Spillover of species between Pt and BaO appears to play an important role in several aspects of the operation of NO_x storage reduction catalysts. Forward and reverse spillover of NO_x species is most obvious during exchange between gaseous and stored NO_x, which is five times faster when Pt and BaO are co-located. Forward spillover is also apparent during NO_x uptake on $Pt/BaO/Al_2O_3$. This is much faster than in systems where the Pt is placed separately from BaO and serves solely to oxidize NO to NO_2, which is taken up by BaO through a slower disproportionation process. Reverse spillover can be inferred during the initial stages of desorption from $Pt/BaO/Al_2O_3$ when the NO_2/NO ratio is much greater than equilibrium, but deactivation of Pt for decomposition of NO_2 is also a factor here. The reduction of stored NO_x is much faster for $Pt/BaO/Al_2O_3$ than for a physical mixture in which the Pt and BaO are separated. The form of spillover here is not so certain. It may involve spillover of hydrogen atoms from metal to BaO, but reverse spillover of NO_x to the metal and reaction to form N_2 appears to be more likely. The major product when NO_x generated by decomposition of stored NO_x is reduced on remotely located Pt

is NH_3, as would be expected from data for the $H_2 + NO$ catalytic reaction when H_2 is in excess, rather than N_2. The present work also shows that NO, which is stored to a minor extent on BaO/Al_2O_3, is present as a species corresponding to NO_2 based on a O:N ratio of 2 in the products of decomposition. NO_2 is stored to a much larger extent and as nitrate based on an O:N ratio of 2.5 in the products of decomposition.

Acknowledgment

This work was supported by a grant from the Australian Research Council.

References

[1] N. Miyoshi, S. Matsumoto, K. Katoh, T. Tanaka, J. Harada, N. Takahashi, K. Yokota, M. Sugiara, K. Kasahara, SAE Technical Paper 950809, 1995.
[2] N. Takahashi, H. Shinjoh, T. Iijima, T. Suzuki, K. Yamazaki, K. Yokota, H. Suzuki, N. Miyoshi, S.-I. Matsumoto, T. Tanizawa, T. Tanaka, S.-S. Tateshi, K. Kasahara, Catal. Today 27 (1996) 63.
[3] W.S. Epling, L.E. Campbell, A. Yezerets, N.W. Currier, J.E. Parks, Catal. Rev. Sci. Eng. 46 (2004) 163.
[4] I. Nova, L. Castoldi, L. Lietti, E. Tronconi, P. Forzatti, F. Prinetto, G. Ghiotti, J. Catal. 222 (2004) 377.
[5] F. Prinetto, G. Ghiotti, I. Nova, L. Castoldi, L. Lietti, E. Tronconi, P. Forzatti, Phys. Chem. Chem. Phys. 5 (2003) 4428.
[6] E. Fridell, H. Persson, L. Olsson, B. Westerberg, A. Amberntsson, M. Skoglundh, Top. Catal. 16–17 (2001) 133.
[7] L. Olsson, H. Persson, E. Fridell, M. Skoglundh, B. Andersson, J. Phys. Chem. B 105 (2001) 6895.
[8] N.W. Cant, M.J. Patterson, Catal. Today 73 (2002) 271.
[9] P. Broqvist, I. Panas, E. Fridell, H. Persson, J. Phys. Chem. B 106 (2002) 137.
[10] J. Despres, M. Koebel, O. Krocher, M. Elsener, A. Wokaun, Appl. Catal. B 43 (2003) 389.
[11] P. Broqvist, H. Gronbeck, E. Fridell, I. Panas, Catal. Today 96 (2004) 71.
[12] J.A. Anderson, B. Bachiller-Baeza, M. Fernandez-Garcia, Phys. Chem. Chem. Phys. 5 (2003) 4418.
[13] S. Kojima, N. Baba, S.-I. Matsunaga, K. Senda, K. Katoh, T. Itoh, SAE Technical Paper 2001-01-1297, 2001.
[14] K.S. Kabin, R.L. Muncrief, M.P. Harold, Catal. Today 96 (2004) 79.
[15] S. Balcon, C. Potvin, L. Salin, J.F. Tempere, G. Djega-Mariadassou, Catal. Lett. 60 (1999) 39.
[16] A. Amberntsson, H. Persson, P. Engstrom, B. Kasemo, Appl. Catal. B 31 (2001) 27.
[17] S. Matsumoto, Y. Ikeda, H. Suzuki, M. Ogai, N. Miyoshi, Appl. Catal. B 25 (2000) 115.
[18] Y.J. Li, S. Roth, J. Dettling, T. Beutel, Top. Catal. 16 (2001) 139.
[19] S. Poulston, R. Rajaram, Catal. Today 81 (2003) 603.
[20] H. Abdulhamid, E. Fridell, M. Skoglundh, Top. Catal. 30–31 (2004) 161.
[21] A.J. Paterson, D.J. Rosenberg, J.A. Anderson, Stud. Surf. Sci. Catal. 138 (2001) 429.
[22] Z. Liu, J.A. Anderson, J. Catal. 224 (2004) 18.
[23] H. Abdulhamid, E. Fridell, M. Skoglundh, Appl. Catal. B 62 (2006) 319.
[24] T. Szailer, J.H. Kwak, D.H. Kim, J.C. Hanson, C.H.F. Peden, J. Szanyi, J. Catal. 239 (2006) 51.
[25] I. Nova, L. Lietti, L. Castoldi, E. Tronconi, P. Forzatti, J. Catal. 239 (2006) 244.
[26] I. Nova, L. Castoldi, L. Lietti, E. Tronconi, P. Forzatti, SAE Technical Paper 2006-01-1368, 2006.
[27] C. Paze, G. Gubitosa, S. Orso Giacone, G. Spoto, F.X. Llabres i Xamena, A. Zecchina, Top. Catal. 30–31 (2004) 169.
[28] T. Uchijima, J.M. Herrmann, Y. Inoue, R.L. Burwell, J.B. Butt, J.B. Cohen, J. Catal. 50 (1977) 464.
[29] S.R. Sashital, J.B. Cohen, R.L. Burwell, J.B. Butt, J. Catal. 50 (1977) 479.
[30] N.W. Cant, M.J. Patterson, submitted for publication.
[31] S.L. Shannon, J.G. Goodwin, Chem. Rev. 95 (1995) 677.
[32] I. Nova, L. Castoldi, F. Prinetto, V. Dal Santo, L. Lietti, E. Tronconi, P. Forzatti, G. Ghiotti, R. Psaro, S. Recchia, Top. Catal. 30–31 (2004) 181.
[33] I. Nova, L. Castoldi, L. Lietti, E. Tronconi, P. Forzatti, SAE Technical Paper 2005-01-1085, 2005.
[34] L. Olsson, E. Fridell, J. Catal. 210 (2002) 340.
[35] S.S. Mulla, N. Chen, L. Cumaranatunge, G.E. Blau, D.Y. Zemylanov, W.N. Delgass, W.S. Epling, F.H. Ribero, J. Catal. 241 (2006) 389.
[36] F. Prinetto, G. Ghiotti, I. Nova, L. Lietti, E. Tronconi, P. Forzatti, J. Phys. Chem. B 105 (2001) 12732.
[37] N.W. Cant, M.J. Patterson, Catal. Lett. 85 (2003) 153.
[38] J. Szanyi, J.H. Kwak, D.H. Kim, S.D. Burton, C.H.F. Peden, J. Phys. Chem. B 109 (2005) 27.
[39] X. Chen, J. Schwank, J. Li, W.F. Schneider, C.T. Goralski, P.J. Schmitz, Appl. Catal. B 61 (2005) 189.
[40] A. Scotti, I. Nova, E. Tronconi, L. Castoldi, L. Lietti, P. Forzatti, Ind. Eng. Chem. Res. 43 (2004) 4522.
[41] D.C. Chambers, D.E. Angove, N.W. Cant, J. Catal. 204 (2001) 11.
[42] D.C. Chambers, Ph.D. thesis, Macquarie University, 2001.
[43] N.W. Cant, D.C. Chambers, I.O.Y. Liu, J. Catal. 231 (2005) 201.
[44] R.J. Gorte, J. Catal. 75 (1982) 164.
[45] R.A. Demmin, R.J. Gorte, J. Catal. 90 (1984) 32.